Bioorganic & Medicinal Chemistry 19 (2011) 894–899

Contents lists available at ScienceDirect

Bioorganic & Medicinal Chemistry

journal homepage: www.elsevier.com/locate/bmc

The effect of structural differences in the reducing terminus of sugars on the binding affinity of carbohydrates and proteins analyzed using photoaffinity labeling

Isao Ohtsuka [a,*], Yutaka Sadakane [a], Mari Higuchi [a], Noriyasu Hada [b], Junko Hada [b], Nobuko Kakiuchi [a], Akiyo Sakushima [a]

[a] School of Pharmaceutical Sciences, Kyushu University of Health and Welfare, 1714-1 Yoshino-cho, Nobeoka City, Miyazaki 882-8508, Japan
[b] Faculty of Pharmacy, Keio University, 1-5-30 Shibakoen, Minato-ku, Tokyo 105-8512, Japan

ARTICLE INFO

Article history:
Received 2 November 2010
Revised 28 November 2010
Accepted 30 November 2010
Available online 4 December 2010

Keywords:
Photoaffinity labeling
Molecular tools
Carbohydrate–protein interaction
Atomic force microscopy (AFM)

ABSTRACT

Because carbohydrates and proteins bind with such low affinity, the nature of their interactions is not clear. Photoaffinity labeling with diazirin groups is useful for elucidating the roles of carbohydrates in these binding processes. However, when carbohydrate probes are synthesized according to this conventional method, the reducing terminus of the sugar is opened to provide an acyclic structure. Because greater elucidation of carbohydrate–protein interactions requires a closed-ring carbohydrate in addition to the photoreactive group, we synthesized new molecular tools. The carbohydrate ligands were synthesized in three steps (glycosylation with allyl alcohol, deprotection, and ozonolysis). Specific binding proteins for carbohydrate ligands were obtained by photoaffinity labeling. Closed ring-type carbohydrate ligands, in which the reducing sugar is closed, bound to lectins more strongly than open ring-type sugars. Carbohydrate to protein binding was observed using AFM.

1. Introduction

Many biological phenomena are initiated by the recognition of carbohydrate ligands by endogenous receptor proteins. Glycosphingolipids and glycoproteins in cell membranes are thought to play especially important roles in a variety of biological events such as extracellular recognition, cell–cell interaction, differentiation, oncogenesis and immunity.[1] Understanding of the role of carbohydrates could lead to the elucidation of many disease mechanisms, but some problems exist in these studies because carbohydrates, in contrast with amino acids and nucleotides, are composed of various complex structures because the configuration of each hydroxyl group, anomeric configuration to be formed in glycosylation reactions and the branching, and often bind with low affinity to proteins.[2] If these problems are addressed, elucidation of the functions of carbohydrates will be accelerated. Formation of a covalent bond to a photoreactive group allows one to maintain the complex between the ligand and its binding protein even under denaturing conditions (Fig. 1).[3] Thus, photoreactive groups function as a powerful hook in fishing for specific binding proteins. The use of the phenyldiazirine group, one of these photoreactive groups, seems promising for achieving efficient crosslinking.[4] Hatanaka synthesized the diazirine units to serve as photoreactive ligands.[5] Because photoreactive units can be easily integrated into physiological ligands such as peptides,[6] proteins,[7] DNA,[8] and carbohydrates[9] by a chemoselective reaction, the biochemist can conjugate these photoaffinity ligands to their physiological ligand of interest.[10] However, when carbohydrate probes are synthesized according to this method, the reducing terminus of the sugar is opened to provide an acyclic structure (**1**, Fig. 2). This ring opening has been confirmed by NMR spectral data.[9] For glycoconjugates with relatively small oligosaccharide, both the reducing and nonreducing end structures are recognized. Oligosaccharides containing a sugar that has been opened on its reducing end are not recognized by proteins (Fig. 3). Therefore, this problem has to be solved by the development of a new method, and the development of such a method will promote further elucidation of carbohydrate-binding protein interactions. In this paper, we report the synthesis of new molecular tools for the elucidation of carbohydrate function (**2**, Fig. 2). These molecular tools contain both closed ring-type carbohydrate ligands, in which the reducing end sugar is closed, and photoreactive diazirine groups for binding to specific proteins. We examined photoreactive ligand structures as potential photoaffinity labels for carbohydrate-binding proteins, and we also investigated the chemical and physical characteristics of carbohydrate-protein binding interactions using atomic force microscopy (AFM).

* Corresponding author. Tel.: +81 982 23 5701; fax: +81 982 23 5702.
E-mail address: ohtsuka@phoenix.ac.jp (I. Ohtsuka).

0968-0896/$ - see front matter © 2010 Elsevier Ltd. All rights reserved.
doi:10.1016/j.bmc.2010.11.067

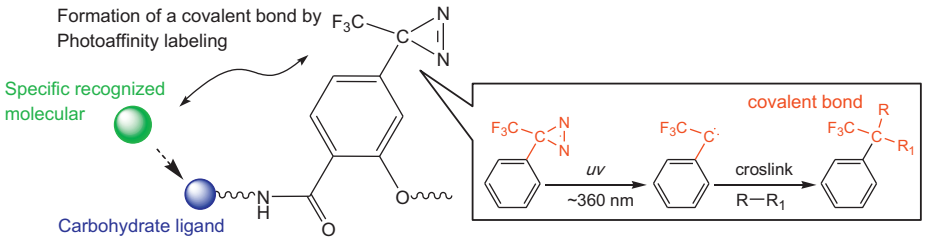

Figure 1. Identification of specific binding molecules for ligands by photoaffinity labeling.

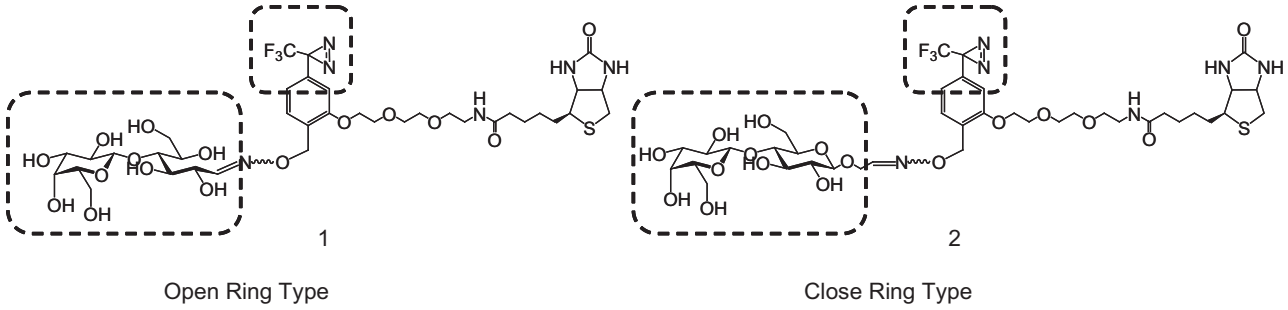

Figure 2. Target molecular tools containing photoreactive group.

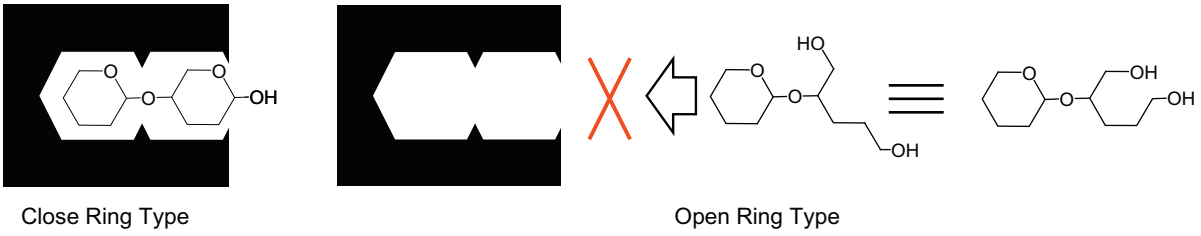

Figure 3. Binding affinity of carbohydrates and proteins are affected by different of the reducing end of sugar.

2. Results and discussion

2.1. Synthesis of carbohydrate ligand 6

Preparation of the designed carbohydrate ligand **6** was straightforward (Scheme 1). We planned a strategy directed to the synthesis of a carbohydrate ligand containing an aldehyde linker. Disaccharide derivative **4** was obtained by condensation of phenyl-2,3,4,6-tetra-*O*-acetyl-β-D-galactopyranosyl-(1→4)-2,3,6-tri-*O*-acetyl-1-thio-β-D-glucopyranoside (**3**),[11] which was prepared by acetylation and thioglysylation of D-lactose. The obtained thioglycoside was then treated with allyl alcohol using *N*-iodosuccimide (NIS) and trifluoromethanesulfonic acid (TfOH) as the glycosylation promoter.[12] After the reaction was completed as indicated by TLC monitoring, the mixture was purified by silica gel column chromatography to give pure product **4** in 76% yield. The β-glycosylated linkage was confirmed by ^{1}H NMR and ^{13}C NMR spectrometry.[13] The anomeric proton of the Glc formed a glycosidic linkage that appeared as a doublet with a homonuclear coupling constant of 7.8 Hz (δ 4.49 ppm, d, 1H, H-1). Allyl group protons were assigned chemical shifts of 5.90 ppm (m, 1H, –C*H*=CH$_2$) and 5.11–5.06 ppm (m, 2H, –CH=C*H*$_2$). The removal of the acetyl groups in **4** was achieved by its treatment with 30% NaOMe in MeOH to give **5**[14] in quantitative

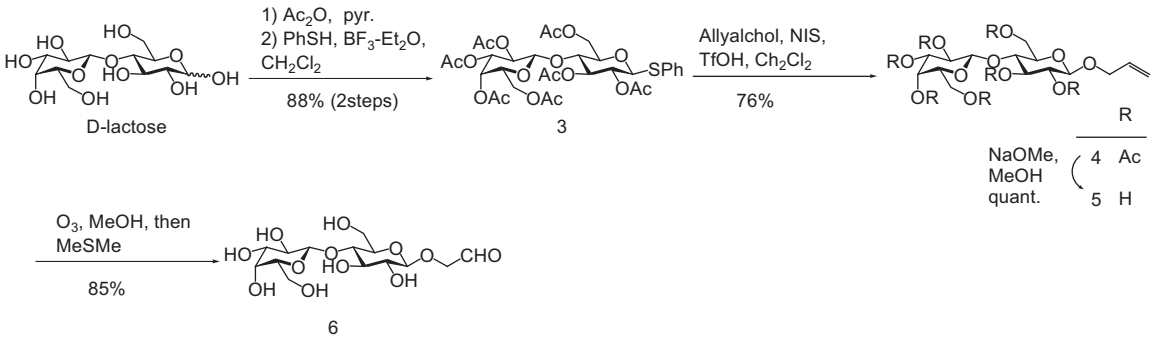

Scheme 1. Syntheis of carbohydrate ligand **6**.

yield. Then selective oxidation to the aldehyde from the alkene in **5** via ozonolysis[15] gave a crude mixture containing **6**.[16] The residue was purified by LH-20 in methanol/water (1:1) to give compound **6** in 85% yield. The structure of carbohydrate ligand **6** was confirmed by ^{1}H NMR and ^{13}C NMR (δ = 79.8 ppm, C-1, δ = 103.5 ppm, C-1′) spectroscopy. The aldehyde group of **6** appeared as a singlet at δ 8.20 ppm (1H, s) by ^{1}H NMR spectrometry, and at 181.4 ppm by ^{13}C NMR spectrometry.

2.2. Synthesis of molecular tools 1 and 2

The oxime group was obtained by coupling the aminooxyl group and aldehyde groups under mild conditions without a promoter. 2-[2-[2-(Biotynylaminoethoxy)-ethoxy]-ethoxy]-4-[3-(trifluoromethyl)-3*H*-diazirin-3-yl]-benzyloxyamine (**8**), which contained the activated aminooxyl group that, was obtained by the removal of the *t*-butoxycarbonyl (Boc) group in affilight-CHO (**7**, Seikagaku Kogyo, Japan; biotin-*N*-bocphenylaminodiazirin), was coupled with compound **6** in acetonitrile/water (3:1), giving the molecular tool containing both a closed ring-type oligosaccharide structure and a diazirin group in quantitative yield (**2**, Scheme 2). Two major peaks were detected by HPLC analysis of the reaction residue, a finding suggested the formation of *E*–*Z* oxime isomers. This mixture was analyzed by ^{1}H NMR, ^{13}C NMR, and HR-FABMS spectrometry. Two triplets at δ = 7.59 ppm and δ = 6.99 ppm were assigned as the oxime protons of the *E*- and *Z*-forms of **2** by ^{1}H NMR spectroscopy.[8] Four doublet peaks were assigned as H-1 (δ = 5.13 ppm, **2**-***Z***, δ = 5.09 ppm, **2**-***E***) and H-1′ (δ = 4.27 ppm, **2**-***E***, δ = 4.22 ppm, **2**-***Z***). The *E*:*Z* ratio of **2** was also determined to be 1.4:1.0 by ^{1}H NMR. HR-FABMS analysis of compounds **2**-***E***, **2**-***Z*** gave a [M+Na]$^+$ ion peak at *m*/*z* 993.3310, in agreement with the formula $C_{39}H_{57}F_3N_6O_{17}SNa$. The structures of **2**-***E***, **2**-***Z*** were confirmed by these analytical results.

The structural heterogeneity of the oxime isomers of the linker might be a synthetic drawback. However, the presence of oxime isomers is likely to be less important for binding photoaffinity labels because the carbohydrate ligands are bound to lectins. In such a case, the separation of each isomer of the photoprobe may not be necessary for the application of this method.

We also synthesized compound **1** using D-lactose in a synthesis similar to that which provided **2**.[9] The structure of **1**-***E***, **1**-***Z*** were confirmed by ^{1}H NMR, ^{13}C NMR and HR-FABMS.

2.3. Elucidation of carbohydrate–protein interactions by photoaffinity labeling

The binding ability of synthetic labeling tools **1** and **2** were examined by photoaffinity labeling to two carbohydrate-binding proteins, SBA and ECA lectins (Fig. 4). The SBA lectin, which is obtained from *Glycine max* (soybean), is known to form the specific binding for D-galactose, D-galactosamine and D-lactosamine.[17] The ECA lectin, which is obtained from *Erythrina cristagalli*, is also known to form the specific binding for D-lactose, D-galactose and D-lactosamine.[18] Thus the both labeling tools **1** and **2** should be bound to both lectins. The labeling tool and lectin protein were mixed and incubated for 30 min at 37 °C, which resulted in promoting the formation of carbohydrate–protein complex. Then, the complex was irradiated with 360 nm ultraviolet light to form the covalent bond between the labeling tool and the lectin. The complex were separated by SDS–PAGE and blotted on polyvinylidene difluoride membrane. The complex were visualized by chemiluminescence of luminol reaction which was induced by horseradish peroxidase (HRP) conjugated with avidin because the labeling tool had a biotin tag.

The results of photoaffinity labeling experiments with synthetic labeling tools **1** and **2** were shown in Figure 5. Molecular mass of complex with SBA and ECA lectin on the membrane were estimated at 32 and 28 kDa, respectively, which were corresponded to the calculated mass of complexes. The labeling tools **2** recognized more strongly both lectins than tools **1** did because dense band were observed in lanes 2 and 6 in comparison with lanes 1 and 5, respectively. These results showed that closed ring-type carbohydrate labeling tool **2** bind to lectins more strongly than open ring-type tool **1**. In both experiments using SBA and ECA lectins, addition of excess amount of lactose inhibited the formation of complex with labeling tool **2** but not that with labeling tool **1** (compare the lanes 1 and 3, 2 and 4, 5 and 7, 6 and 8). These competition experiments showed that only labeling tool **2** recognized carbohydrate binding site of the lectin. Taken together, the cyclic form of carbohydrates is important to perform the photoaffinity labeling with carbohydrate ligands.

2.4. AFM images of carbohydrate and specific binding protein using photoaffinity labeling

The investigation of the chemical and physical characteristics of carbohydrate–protein interactions must elucidate the functions of carbohydrate.[19] AFM enables the observation of their surfaces on the nanoscale level to give insight about their characteristics. A mixture of molecular tool **2** and SBA lectin was incubated (sample A) and that irradiated with UV (sample B). Any changes in the morphology of the surface were observed by AFM. The surfaces of lectins were flat before UV irradiation (sample A: Fig. 6A), but dot patterns appeared on them after UV irradiation (sample B: Fig. 6B). These findings indicated that UV irradiation promoted covalent

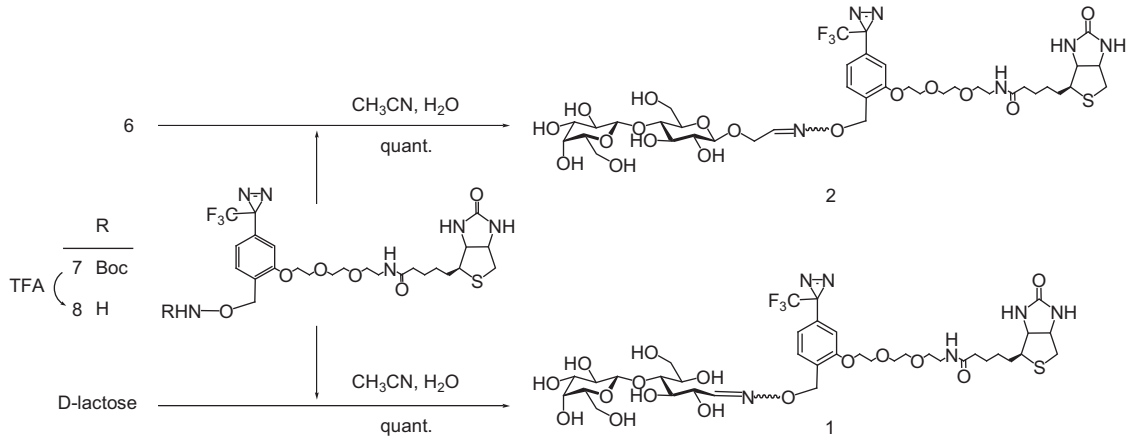

Scheme 2. Synthesis of molecular tools 1 and 2.

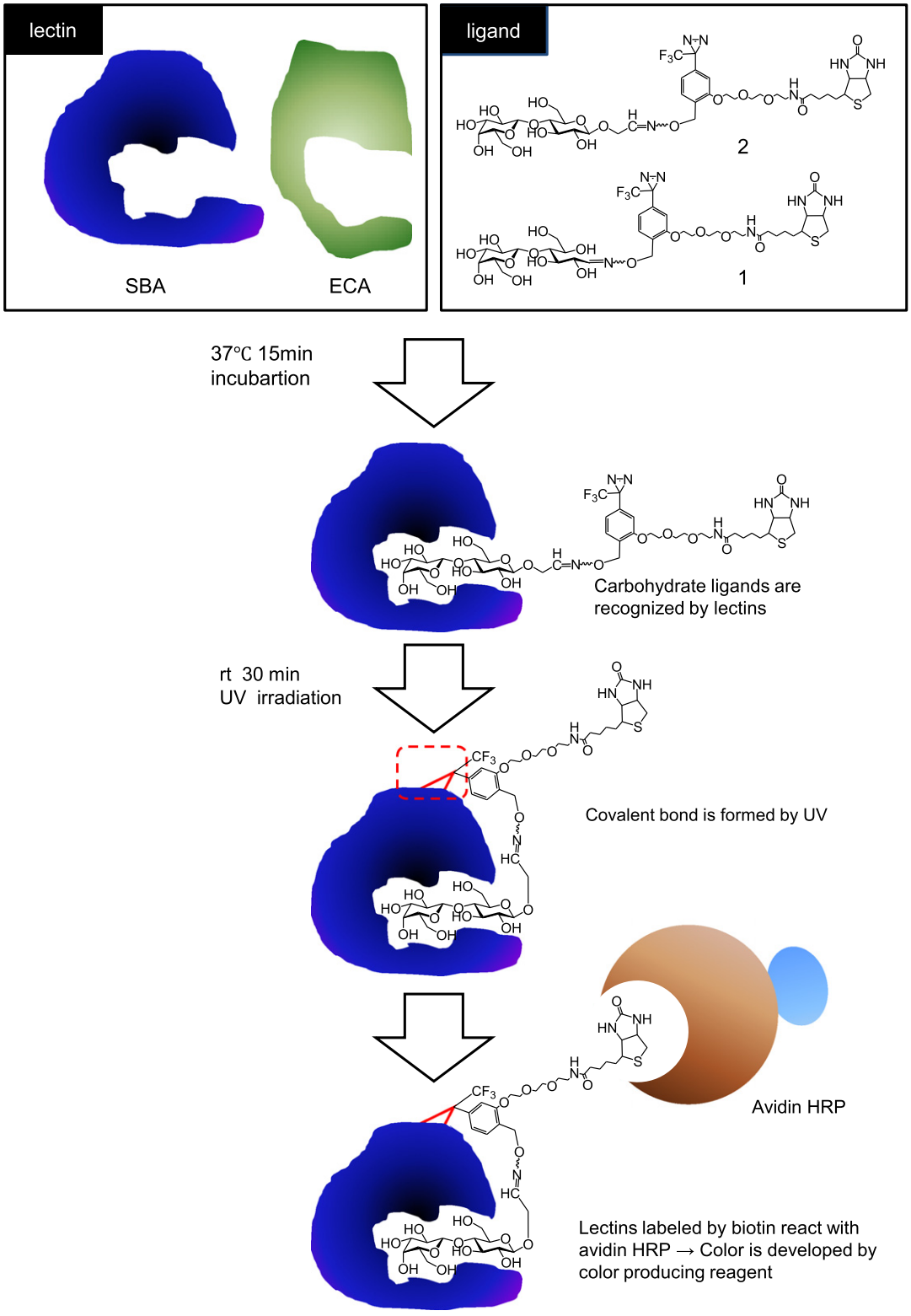

Figure 4. Elucidation of molecular tools (**1**, **2**) and specific binding lectin for D-lactose (SBA, ECA) interactions by photoaffinity labeling.

bond formation between **2** and the lectins. Thus, these dots on the mountain-like structure imply ligand binding. Because the molecular size of one SBA lectin is 31 kDa, and amino acids residue of it is 285 A.A.,[17] these images suggested that SBA lectin contains many binding sites for D-lactose. These results provide useful insight for the elucidation of the physical characteristics of SBA lectin.

3. Conclusion

In summary, new molecular tools for the elucidation of carbohydrate roles were developed. These tools featured both a closed ring-type sugar and a photoactive phenyldiazirine group. We showed that the structural difference between closed ring- and open ring-type carbohydrates affected binding affinity to proteins.

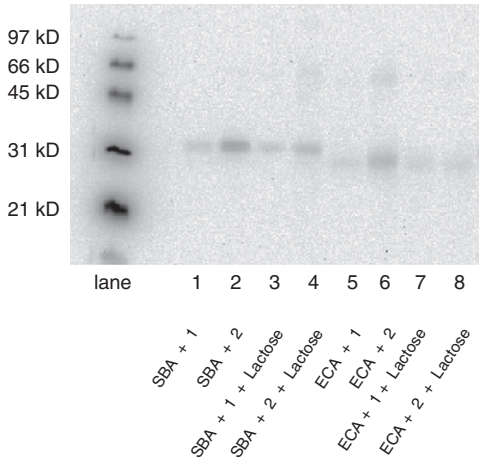

Figure 5. SDS–PAGE analysis of binding affinity of carbohydrates and proteins.

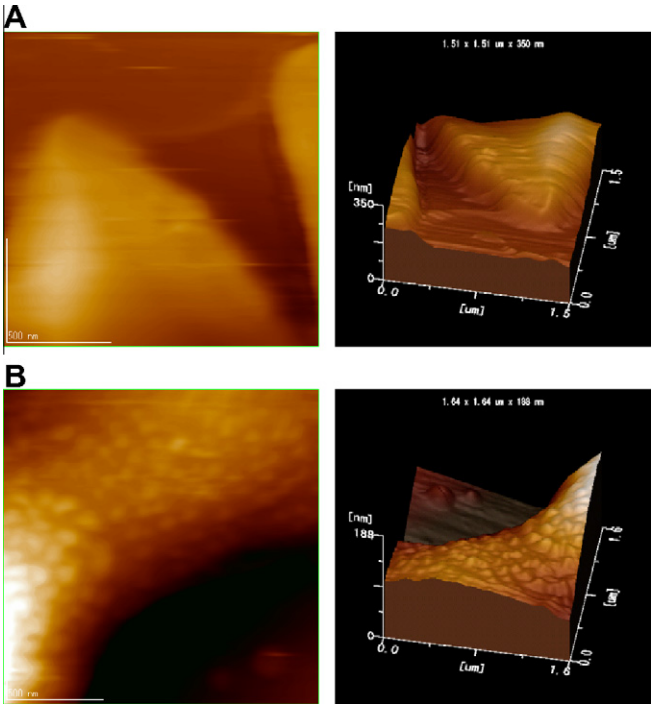

Figure 6. AFM Image of compound **2** and SBA lectin: (A) before UV irradiation (sample A) and (B) after UV irradiation (sample B). Each mount areas are lectin sites. Scan area: 1.5 × 1.5 μm.

This study confirmed that carbohydrate structure, in both non-reducing end and reducing end sugars, is deeply related to the recognition event between carbohydrates and proteins. These molecular tools also enable further elucidation of the various carbohydrate-binding protein interactions by substituting for the carbohydrate ligand in binding studies. As a result, they will be used in future studies to elucidate carbohydrate functions on cell surfaces.

4. Experimental

4.1. General method

^{1}H NMR and ^{13}C NMR spectra were measured with a JMN AL 400 FT NMR spectrometer (JEOL Ltd) with Me_4Si as the internal standard for solutions in $CDCl_3$, D_2O and CD_3OD. ESI mass spectrometry were measured on a LCQ Advantage (Thermo Fisher Scientific Ltd). High-resolution mass spectrometry were measured on a JMS-700 (JEOL Ltd) under FAB condition. TLC was performed on silica gel 60 F254 (E. Merk) with detection by quenching UV fluorescence and by charring with 10% H_2SO_4. Column chromatography was carried out on silica gel 60 (E. Merk). AFM images were observed using JSPM-5200 (JEOL Ltd).

4.2. Chemistry

4.2.1. 2-Oxyoethyl β-D-garactopyranosyl-(1→4)-β-D-glucopyranoside (6)

Ally glycoside **5** (0.62 mg 160 μmol) was dissolved in MeOH (10 mL). The solution was cooled to −78 °C and then treated with ozone and oxygen gas by bubbling until the solution remained blue. After 10 min, the ozone was evacuated with nitrogen for 15 min at −78 °C, and dimethyl sulfide (1.0 mL) was added. The resulting solution was allowed to warm to room temperature over 1 h. The clear solution was concentrated and purified using Sephadex LH-20 column chromatography (H_2O/MeOH = 1:1 as the eluent) to give **6** (52 mg, 85%). ^{1}H NMR (400 MHz, $CDCl_3$) δ 8.20 (s, 1H, –CHO), 4.74 (d, J = 7.8 Hz, 1H, H-1), 4.22 (d, J = 7.8 Hz, 1H, H-1′), 3.69 (t, 1H, H-3′), 3.58–3.41 (m, 11H), 3.30 (t, J = 9.6 Hz, 1H, H-2′), 3.20 (t, J = 7.1 Hz, 1H, H-2); ^{13}C NMR (400 MHz, $CDCl_3$) δ 181.4 (–CHO), 103.5 (C-1′), 79.8 (C-1), 78.4, 77.0, 76.0, 75.7, 73.2, 72.2 (C-2), 71.6 (C-2′), 69.3 (C-3′), 61.7, 60.6; HR-MS (FAB) calcd for $C_{14}H_{25}O_{12}^+$ $(M+H)^+$ m/z 385.1346; measure m/z 385.1346.

4.2.2. 2-Oxyoethyl β-D-garactopyranosyl-(1→4)-β-D-glucopyranoside-*O*-2-[2-[2-(biotynylaminoethoxy)-ethoxy]-ethoxy]-4-[3-(trifluoromethyl)-3*H*-diazirin-3-yl]-benzyloxime (2-*E*, 2-*Z*)

2-[2-[2-(Biotynylaminoethoxy)-ethoxy]-ethoxy]-4-[3-(trifluoromethyl)-3*H*-diazirin-3-yl]-benzyloxycarbanic acid *tert*—butyl ester (AffiLight—CHO, Seikagaku corporation) (**7**) (5 mg, 7.3 μmol) was dissolved in CH_2Cl_2 (70 μL). To this solution was added trifluoroacetic acid (70 μL) at 0 °C, and the mixture was stirred for 1 h. Toluene (100 μL) was added to the reaction mixture, and it was then concentrated by nitrogen flash. Triethylamine (18 μL) was added to the residue and then concentrated to give **8**.

To a solution of **8** (4.4 mg, 7.3 μmol) in CH_3CN (255 μL) was added **6** (4.2 mg, 11 μmol) in H_2O (85 μL), and the resulting mixture was shaken for 1 h at room temperature. The mixture of **2-*E*** and **2-*Z*** (7.1 mg, quant.) was purified by reversed-phase HPLC using a C18 column, Shiseido Capcell Pack C18 UG120 (20 mm i.d. × 250 mm, Shiseido Co. Ltd, Japan, with a linear gradient of 0–80% acetonitrile, 0.1% TFA at a flow rate of 1 mL/min, with monitoring at 215 nm). ^{1}H NMR (400 MHz, CD_3OD) δ 7.59 (t, 1H, CH═NO of **2-*E***), 7.49 (t, 1H), 7.36 (d, J = 7.8 Hz, 1H), 6.99 (br t, 1H, –CH═NO of **2-*Z***), 6.88 (br d, 1H), 6.74 (br s 1H), 5.13 (s, 1H), 5.09 (s, 1H), 4.47 (d, 1H, –OC*H*$_2$CH═NO of **2-*Z***), 4.34 (d, 1H, –OC*H*$_2$CH═NO of **2-*E***), 4.27 (d, 1H, H-1′ of **2-*E***), 4.22 (d, 1H, H-1′ of **2-*Z***), 4.17 (d, 2H, CH═NOC*H*$_2$– × 2 of **2-*Z***), 3.86 (d, 2H, CH═NOC*H*$_2$– × 2 of **2-*E***); ^{13}C NMR (400 MHz, $CDCl_3$) δ 139.7, 119.9, 77.0, 74.8, 71.8, 71.3, 70.6, 70.3, 63.3, 61.6, 56.9, 41.1, 40.3, 36.7, 29.8, 29.5, 26.8, 15.8; HR-MS (FAB) calcd for $C_{39}H_{57}F_3N_6O_{17}SNa^+$ $(M+Na)^+$ m/z 993.3351; measure m/z 993.3310.

4.2.3. 2-Oxyoethyl β-D-garactopyranosyl-(1→4)-β-D-glucopyranoside-*O*-2-[2-[2-(biotynylaminoethoxy)-ethoxy]-ethoxy]-4-[3-(trifluoromethyl)-3*H*-diazirin-3-yl]-benzyloxime (1-*E*, 1-*Z*)

To a solution of **7** (4.4 mg, 7.3 μmol) in CH_3CN (255 μL) was added D-lactose (5.4 mg, 11 μmol) in H_2O (85 μL), and the resulting mixture was shaken for 1 h at room temperature. The mixture of **1-*E*** and **1-*Z*** (9 mg, quant.) was purified by reversed-phase HPLC using a C18 column, Shiseido Capcell Pack C18 UG120 (20 mm i.d. × 250 mm, Shiseido Co. Ltd, Japan, with a liner gradient of

0–80% acetonitrile, 0.1% TFA at a flow rate of 1 mL/min, with monitoring at 215 nm). ^{1}H NMR (400 MHz, CD_3OD) δ 7.47 (t, 1H, CH═NO of **1**-***E***), 7.38 (t, 1H, –CH═NO of **1**-***Z***), 6.88 (br d, 1H), 6.74 (br s 1H), 5.14 (s, 1H), 5.08 (s, 1H), 4.36 (d, 1H, J = 7.8 Hz, H-1′ of **1**-***Z***), 4.29 (d, 1H, J = 7.8 Hz, H-1′ of **1**-***E***); ^{13}C NMR (400 MHz, $CDCl_3$) δ 130.6, 130.3, 119.9, 110.5, 104.9, 77.0, 74.7, 72.5, 71.8, 71.2, 70.6, 70.5, 70.2, 69.5, 63.3, 61.6, 56.9, 49.6, 40.3, 36.7, 29.7, 29.5, 26.8; HR-MS (FAB) calcd for $C_{37}H_{55}F_3N_6O_{16}SNa^+$ $(M+Na)^+$ m/z 951.3245; measure m/z 951.3203.

4.3. Analysis of binding affinity of carbohydrates and lectins by photoaffinity labeling

The lectins (2.5 μg) were obtained from Soybean, *G. max* and *E. cristagalli* (J-Oil Mills Co. Ltd, Japan) and incubated with photoreactive carbohydrates **1** and **2** in 50 mM phosphate buffer (pH 7.4) at 37 °C for 10 min in the dark. In the case of competitor experiments, 50 mM lactose was pre-incubated with the solution of lectins for 15 min at 37 °C before the addition of photoreactive carbohydrates. Specimens were then irradiated at 0 °C for 30 min with a 30-watt long-wavelength UV lamp to promote crosslinking. The irradiated samples were subjected to SDS–PAGE (12% polyacrylamide gel) and transferred to a PVDF membrane. Biotinylated carbohydrates on the membrane were then visualized by chemiluminescent detection with avidin-horseradish peroxidase (HRP) conjugate.

4.4. AFM observation

Sample A—1.0 mM compound **2** in water (2.5 μL), 1.0 mM SBA lectin in water (2.5 μL) and 0.5 M phosphate buffer (pH 7.6) (5.0 μL) were dissolved in water (30 μL).

Sample B—1.0 mM compound **1** in water (2.5 μL), 1.0 mM SBA lectin in water (2.5 μL) and 0.5 M phosphate buffer (pH 7.6) (5.0 μL) were dissolved in water (30 μL).

Solutions of sample A and B (0.1 μL) were added dropwise to a freshly cleaved mica plate (5.0 × 5.0 mm) and dried for observation by AFM. The AFM probe used was a Micro Cantilever CSC38 (JEOL Ltd) made of silicon and coated with Au, which had a spring constant of 0.08 N/m, a length of 250 μm, and a thickness of 1.0 μm. The AFM observation was carried out with the contact mode in the air at 25 °C.

Acknowledgements

This study was supported by Mitsubishi Chemical Corporation Fund to I.O., and by Grant-in-Aid for Scientific Research from the Ministry of Education, Culture, Sports, Science and Technology of Japan to Y.S.

Supplementary data

Supplementary data associated with this article can be found, in the online version, at doi:10.1016/j.bmc.2010.11.067.

References and notes

1. Taylor, M. E.; Drickamer, K. *Introduction to Glycobiology*; Oxford Univ. Press: New York, 2003.
2. (a) Lee, Y. C. *Ciba Found. Symp.* **1989**, *145*, 80–95; (b) Weis, W. I.; Drickamer, K. *Ann. Rev. Biochem.* **1996**, *65*, 441–473; (c) Rini, J. M. *Annu. Rev. Biophys. Biomol. Struct.* **1995**, *24*, 551–557.
3. Hatanaka, Y.; Sadakane, Y. *Curr. Top. Med. Chem.* **2002**, *2*, 271–288.
4. Hatanaka, Y.; Nakashima, H.; Kanaoka, Y. *Rev. Heteroat. Chem.* **1996**, *14*, 213–243.
5. Hatanaka, Y. *J. Synth. Org. Chem. Jpn.* **1998**, *56*, 53–62.
6. Nakashima, H.; Hashimoto, M.; Sadakane, Y.; Tomohiro, T.; Hatanaka, Y. *J. Am. Chem. Soc.* **2006**, *128*, 15092–15093.
7. Sadakane, Y.; Takagi, T.; Tomohiro, T.; Tsurusawa, K.; Konoha, K.; Kawahara, M.; Hatanaka, Y. *Photomed. Photobiol.* **2004**, 35–40.
8. O'Neil, K. T.; Wolfe, Jr. H. R.; Erickson-Viita-nen, S.; Degra, W. F. *Science* **1987**, *236*, 1454–1456.
9. Hatanaka, Y.; Kempin, U.; Jong-Jip, P. *J. Org. Chem.* **2000**, *65*, 5639–5643.
10. (a) Koshi, Y.; Nakata, E.; Hamachi, I. *Org. Biomol. Chem.* **2005**, *6*, 1349–1352; (b) Fleming, S. A. *Tetrahedron* **1995**, *51*, 12479–12520; (c) Fang, K.; Hashimoto, M.; Jockusch, S.; Turro, N. J.; Nakanishi, K. *J. Am. Chem. Soc.* **1998**, *120*, 8543–8544.
11. Sun, B.; Pukin, A. V.; Visser, G. M.; Zuilhof, H. *Tetrahedron Lett.* **2006**, *47*, 7371–7374.
12. Veeneman, G. H.; van Boom, J. H. *Tetrahedron Lett.* **1990**, *31*, 1331–1334.
13. Matsuoka, K.; Terabatake, M.; Umino, A.; Esumi, Y.; Hatano, K.; Terunuma, D.; Kazuhara, H. *Biomolecules* **2006**, *7*, 2274–2283.
14. Okamoto, K.; Kondo, T.; Goto, T. *Tetrahedron* **1987**, *43*, 5919–5928.
15. Sun, X.-L.; Kanie, Y.; Guo, C.-T.; Kanie, O.; Suzuki, Y.; Wong, C.-H. *Eur. J. Org. Chem.* **2000**, 2643–2653.
16. Kononov, L. O.; Cheshev, P. E.; Nifant'ev, N. E. *Russ. Chem. Bull.* **2000**, *7*, 1305–1309.
17. (a) Lis, H.; Sharon, N. *J. Biol. Chem.* **1978**, *253*, 3468–3476; (b) Vodkin, L. O.; Rhodes, P. R.; Goldberg, R. B. *Cell* **1983**, *34*, 1023–1031; (c) Buts, L.; Dao-Thi, M. H.; Loris, R.; Wyns, L.; Etzler, M.; Hamelryck, T. *J. Mol. Biol.* **2001**, *309*, 193–201; (d) Olsen, L. R.; Dessen, A.; Gupta, D.; Sabesan, S.; Sacchettini, J. C.; Brewer, C. F. *Biochemistry* **1997**, *36*, 15073–15080; (e) Dessen, A.; Gupta, D.; Sabesan, S.; Brewer, C. F.; Sacchettini, J. C. *Biochemistry* **1995**, *34*, 4933–4942; (f) Galbraith, W.; Goldstein, I. J. *FEBS Lett.* **1970**, *9*, 197–201; (g) Jaffe, C. L.; Ehrlich-Rogozinski, S.; Sharon, N. *FEBS Lett.* **1977**, *82*, 191–196.
18. (a) Iglesias, J. L.; Lis, H.; Sharon, N. *Eur. J. Biochem.* **1982**, *123*, 247–252; (b) Itakura, Y.; Nakamura-Tsuruta, S.; Kominami, J.; Sharon, N.; Kasai, K.; Hirabayashi, J. *J. Biochem.* **2007**, *142*, 459–469; (c) Svensson, C.; Teneberg, S.; Nilsson, C. L.; Kjellberg, A.; Schwarz, F. P.; Sharon, N.; Krengel, U. *J. Mol. Biol.* **2002**, *321*, 69–83.
19. Ohtsuka, I.; Yokoyama, S. *Chem. Pharm. Bull.* **2005**, *53*, 42–47.